NUMERICAL SIMULATION OF THE FLOW IN AN ARTERIAL BLOOD FILTER

Bernardo Augusto Roca Arenales, bernardo.arenales@gmail.com
Pedro Salomé de Oliveira, pesalome@ufmg.br
Rudolf Huebner, rudolf@ufmg.br
Marcos Pinotti Barbosa, pinotti@demec.ufmg.br
Ramon Molina Valle, ramon@demec.ufmg.br
Universidade Federal de Minas Gerais – Departamento de Engenharia Mecânica
Campus Pampulha – Av. Presidente Antônio Carlos, 6627 – CEP 31270-901 – Belo Horizonte – MG - Brasil

Abstract. *Cardiopulmonary bypass with extracorporeal blood oxygenation has become one of the most frequently performed classes of procedures worldwide. Cerebral damages after cardiac operations have been widely recognized since the early days of open-heart surgery and it happens because emboli are introduced into the patient's arteries. Interposition of a filter in the arterial line of the extracorporeal circuit has been one of the proposed methods for avoiding cerebral damage during a cardiopulmonary bypass. The presence of the blood filter will induce a resistance to the blood flow and this resistance can be described in terms of pressure drop across the arterial blood filter and its level must be kept below a threshold value otherwise red blood cells will be damaged. The aim of this work is to evaluate the pressure drop across arterial blood filter and visualize the global flow structure inside the filter. A test bench was developed and visual tests and pressure drops were measured at different flow rates. Finally the flow across the filter was simulated and numerical results were compared with the experimental data. Results shown a good agreement between both methodologies.*

Keywords*: Blood Filter, Flow, Pressure Drop, Simulation, Experimental*

1. INTRODUCTION

Nowadays cardiopulmonary bypass (CPB) with extracorporeal blood oxygenation is a very common practice. Microembolization occurs during CPB due to the presence of bubbles air, thrombi, platelet aggregates and pieces of plastic into the arterial line as cited by Waaben *et al.* (1994). Microemboli can cause organ dysfunction, especially in the brain, liver, lung and kidney. The use of a blood filter in the arterial line of the extracorporeal circuit has been one of the proposed methods to retain microemboli thus avoiding organ dysfunction.

Interposition of a filter in the arterial line of the extracorporeal circuit has been one of the proposed methods to avoid cerebral damage during CPB (Aris et all., 1986). The use of these filters has increased in the last years. Accordingly Mueller et all. (1999), three reasons seem to justify the systematic use of arterial line filters.

- They are excellent gross bubble traps,
- There is an increasing evidence that membrane oxygenators are associated with significant reduction, but not complete elimination, of microbubbles delivered to the patient,
- And finally, their wide use suggests that there is a little adverse effect from their use.

The use of an arterial line filter has also some disadvantages. A pressure gradient can be built up across the filter inducing a switch to an external bypass line. There is also a risk for air embolism because air trapped in the filter during initial filling may be ejected later into the patient. Finally line filters may damage blood elements. Although the foci of thrombus formation and embolization in the arterial filter were recognized, no quantitative information about rate, size and amount of emboli shed from the filter, nor about the interrelationship of trapping of emboli in the arterial filter and thrombi formed and emboli shed from arterial filter is available (Dewanjee et all., 1992).

The analysis of flow through the arterial blood filter and its effect over the blood cells constitute an essential tool to the development of arterial blood filters. The development of blood filters available in the market have been made by the trial and error method which is a long, expensive and inefficient process. Flow analysis techniques used in engineering can be a great support in the project of blood filters. The flow analysis have been done through experiments or by the use of numerical solutions. Andrade *et al.* (1997) made use of a flow visualization technique to improve the project of a blood pump. Pinotti e Paone (1996) used the laser Doppler anemometry technique to study the flow inside a blood pump and estimate the damage occurred due to it. Castellini et al. (2004) made use of the particle image velocimetry to evaluate the flow in a cardiac valve. Huebner (2003) utilized flow visualization technique by dye injection, Laser Doppler anemometry and Particle Image Velocimetry to evaluate the flow of several blood filters produced in Brazil. Burgreen *et al.* (2004) and Untaroiu *et al.* (2005) made use of flow visualization techniques in conjunction with numerical simulations to evaluate the flow in a ventricular assistance device. Gage *et al.* (2002) and Gartner *et al.* (2000) evaluated the flow in membrane oxygenators using computational fluid mechanics. It can be noticed that the use of numerical simulations together with experimental techniques can be usefull in the development of devices like blood pumps, oxygenators and arterial blood filters.

The aim of the present work in to evaluate the pressure drop across an arterial blood filter. A test bench was developed and a solution of water and glycerin was used as working fluid. Finally the pressure drop was analyzed numerically and the results compared with the experimental data.

2. METHODOLOGY

2.1. The Blood Filter

The filter studied is used in cardiopulmonary bypass procedures. The filter is made of acrylic and polyester is used in the filtering element. The filtering element has a porosity of 40 μm. The filter inlet and outlet connectors have a diameter of 9,5 mm and are made of reinforced acrylic. The filter is projected to be used in adult patients and can be operated with a maximum flow rate of 6 liters per minute. It has a bypass line that can be used in situations where the filtering element pores are closed and another line is used to eliminate air trapped by the filter. Figure 1 shows a schematic view of the tested filter, its elements and how it works. In figures 1, blue arrows are used to indicate unfiltered blood while red arrows indicate filtered blood.

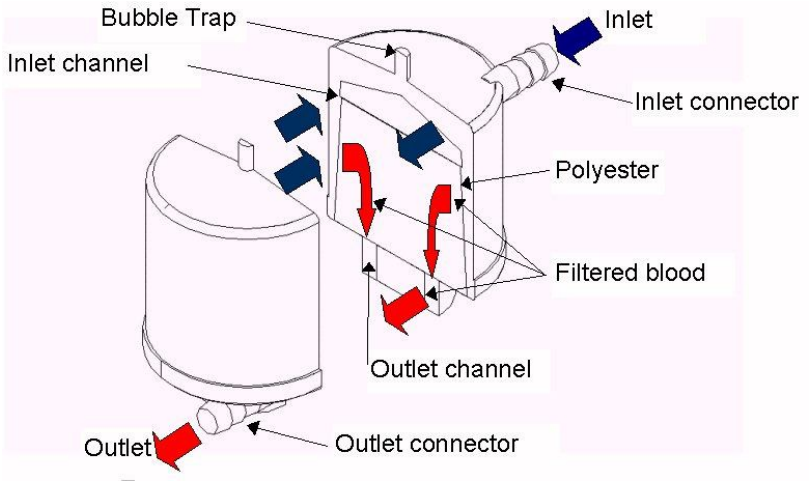

Figure 1. Schematic view of the filter

In this filter blood flows through the inlet connector, located at the upper part of the filter, and describes a descending helical movement while it flows along the inlet channel. During this helical movement the blood flows through the filtering element, reaches the outlet channel and flows in direction of the outlet connector, located at the bottom of the filter.

2.2 Numerical Model

The flow can be modeled by the Reynolds-averaged Navier-Stokes equations (Ilinca et al., 1997):

Continuity equation

$$\nabla.\vec{u} = 0 \tag{1}$$

where, $\vec{u}$ represents the velocity vector.

Momentum equation

$$\rho\vec{u}.\nabla\vec{u} = -\nabla p + \nabla.\left[(\mu + \mu_T)(\nabla\vec{u} + \nabla\vec{u}^T)\right] \tag{2}$$

where ρ represents the density, p the pressure, $\vec{u}$ the velocity vector, μ the fluid viscosity and μ_T the turbulent viscosity.

There are many two-equation models used in practice today. Among them is the k-ε model, which has been used most frequently for low-speed incompressible flows in isotropic turbulence (Chung, 2002). In this model the turbulent viscosity is computed as

$$\mu_T = \bar{\rho} c_\mu \frac{k^2}{\varepsilon} \tag{3}$$

The system is closed by including the transport equations for k and ε,

$$\rho \vec{u}.\nabla k = \nabla.\left[\left(\mu + \frac{\mu_T}{\sigma_k}\right)\nabla k\right] + \mu_T P(\vec{u}) - \rho\varepsilon \tag{4}$$

$$\rho \vec{u}.\nabla \varepsilon = \nabla.\left[\left(\mu + \frac{\mu_T}{\sigma_\varepsilon}\right)\nabla \varepsilon\right] + C_1 \frac{\varepsilon}{k} \mu_T P(\vec{u}) - C_2 \rho \frac{\varepsilon^2}{k} \tag{5}$$

where the production of turbulence is defined as

$$P(\vec{u}) = \nabla \vec{u}.\left(\nabla \vec{u} + \nabla \vec{u}^T\right) \tag{6}$$

The constants C_μ , C_1, C_2, σ_k e σ_ε values are those proposed by Launder and Spalding (1972). The value of each constant is shown on table 1.

Table 1. Constants values for the K-ε turbulence model

C_μ = 0,09	**C_1=1,44**	**C_2=1,92**	**σ_κ=1,00**	**σ_ε=1,30**

The boundary conditions for inlet were defined with a pressure reference, subsonic flow regime and k-ε turbulent flow. Values of k and ε were evaluated accordingly the equations (7) and (8) (Versteeg e Malalasekera, 1995).

$$k = \frac{3}{2}\left(U_{ref} T_i\right)^2 \tag{7}$$

$$\varepsilon = c_\mu^{3/4} \frac{k^{3/2}}{0{,}07L} \tag{8}$$

where U_{ref} is the average velocity along the inlet section, L is a characteristic length, in this case the connector diameter and T_i is the turbulence intensity equal to 5%. The boundary conditions for walls were the no slip. For the outlet, the boundary conditions defined with subsonic flow regime and mass flow rate accordingly the flow simulated.

The effect of the filtering element was simulated using Darcy law (Gage *et al.* 2002). The pressure drop is included in the source term of the momentm equation along the radial direction.

$$\Delta P = \frac{\mu}{K_p} \cdot V \tag{9}$$

where P is the mean static pressure, μ is the dynamic viscosity , K_p is the permeability of the porous media e V is the superficial velocity.

Simulations were performed considering a working fluid with transport properties similar those of the blood during extracorporeal circulation. The simulations were performed considering flow rates of 1.5, 3.0 and 4.5 l/min and the results compared with experimental data.

The SOLIDWORKS™ software was used to generate a virtual model of this filter, including every component. Three different volumes were created: the region where the blood flows before the filtration, the filtering element and the region where the filtered blood flows. A small extension was added to the entrance and exit connectors, attempting to approximate the real conditions of the flow. The volumes were exported to the ANSYS™ Workbench which generated the meshes of each part of domain. The software used to perform the numerical simulation was the CFX™ V11.0. Figure 2 shows an overview of the mesh at the surface of domain.

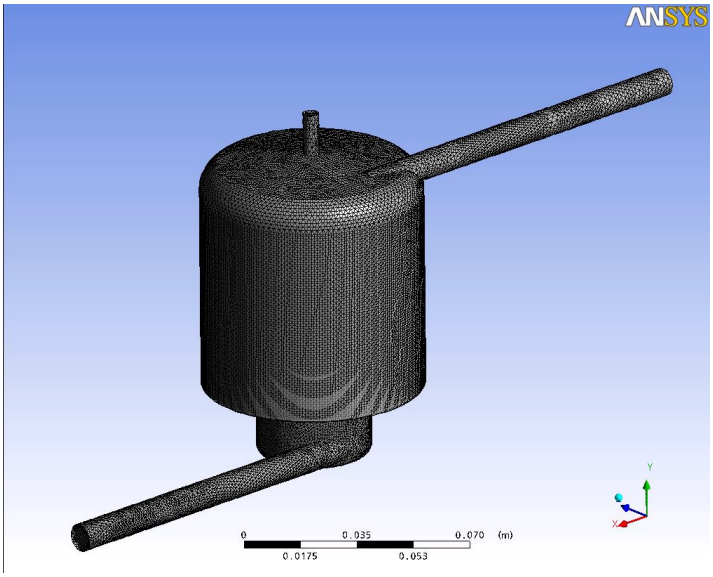

Figure 2. Overview of discretized domain

Figure 3 shows details of the mesh. At the left side, it can be seen the detail of the attachment of inlet connector with the filter body. At the right side, it is possible to notice the fine grid near the wall surrounding the exit connector. This fine grid was applied in the generation of every solid surface of domain, making the pressure drop more accurate.

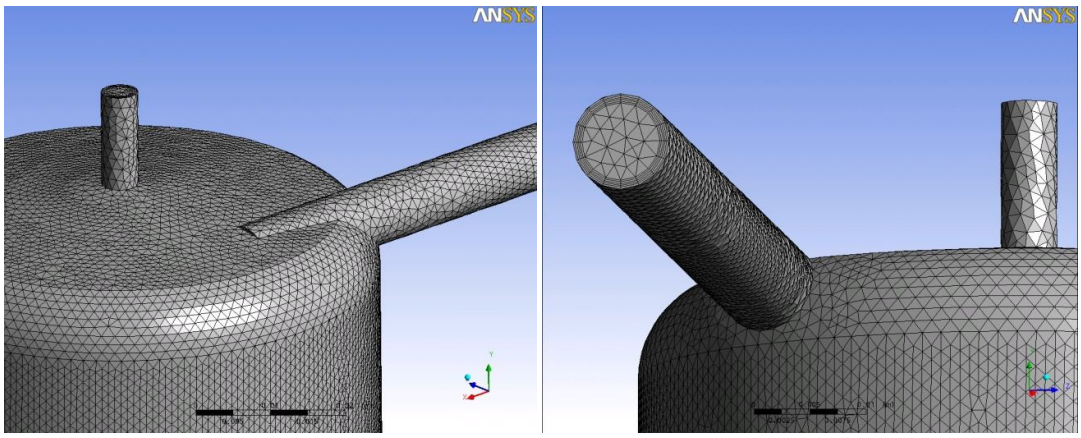

Figure 3. Mesh details

Figure 4 shows the mesh used in the filtering element and at the outlet channel.

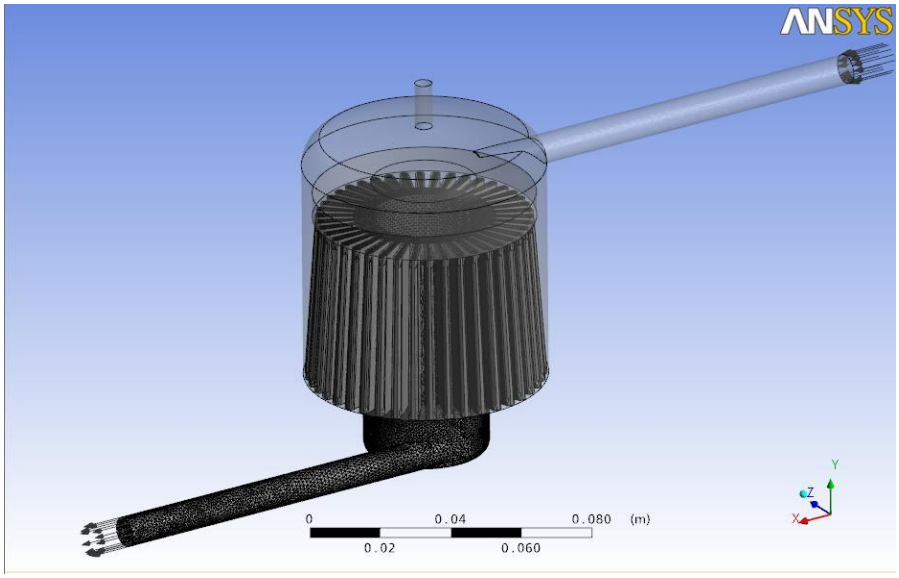

Figure 4. Mesh used in the filtering element and at the outlet channel.

A convergence criterion of 10^{-4} was adopted to the root mean square of the residual (rms) considering all domain. The last simulation has used a mesh with 600.000 nodes.

2.3 The Test Bench

A test bench was assembled in order to reproduce the flow condition observed during a cardiopulmonary bypass. Figure 5 depicts schematically the test circuit.

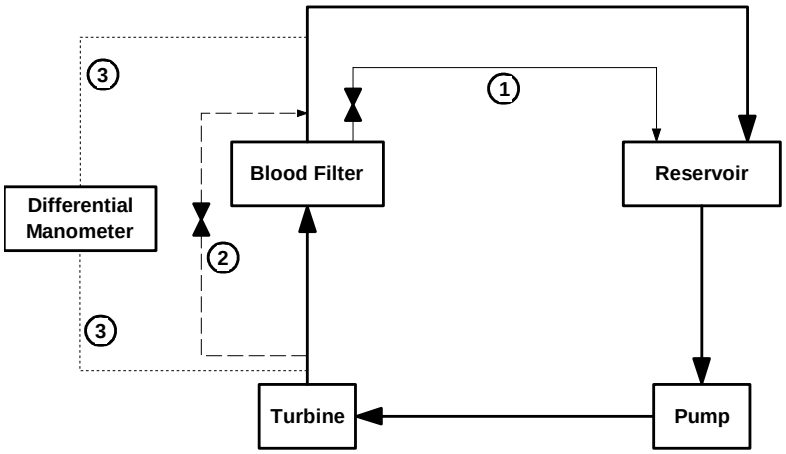

Figure 5 – Schematic view of the test circuit

Working fluid was pumped through the turbine and blood filter returning to the circuit reservoir. Line 1 represents the bubble trap and was used during the circuit filling up. Pressure drop across the filter was monitored by a differential manometer, indicated by the dotted lines 3. Flow rate was monitored by a turbine flow meter and the pump rotating speed was controlled changing the input voltage of a brushless motor. All elements were connected using PVC flexible tubes.

The pressure drop was measured changing the flow rate and reading the differential pressure in the manometer. The flow rate varies in a range of 1.5 to 4.5 l/min, with an increment of 0.5 l/min. Tests were performed in a non-pulsatile condition and a solution of water and glycerin, with glycerin concentration of 40%, in mass, was used as working fluid.

3. RESULTS

Figure 5 shows the location of the four planes (N, S, O and E) used in the results analysis.

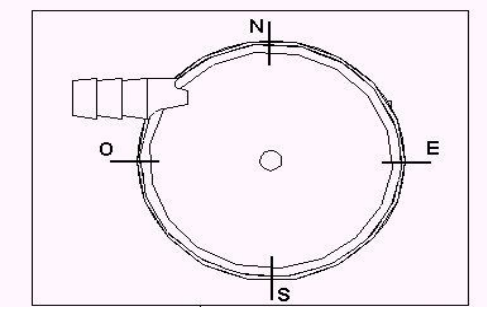

Figure 5. Top view of the filter showing the planes positions

Figure 7 shows flow streamlines inside the filter. The color variation indicates a maximum velocity of 2.12 m/s near the outlet conector.

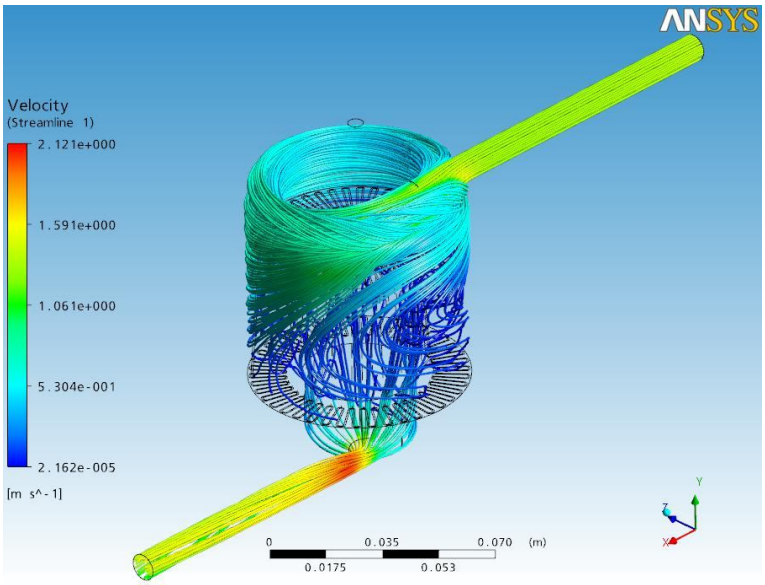

Figure 7. Streamlines along filter and velocity vectors on a horizontal plane

The flow enters the filter and hits the opposite wall and the the main flow moves downward, clockwise. Near the outlet connector is noticeable a flow division where a part of it moves clockwise. These results follow the pattern obtained on visualization tests with coloring injection made by Huebner [2003], shown on figure 8.

Figure 8. Top view showing the flow direction and the division at the exit connector neighborhood (Huebner, 2003)

Figure 9 shows velocity vectors along planes N and S. At plane N, it can be seen a presence of a jet coming from the entrance connector and a flow pattern moving clockwise inside the filter.

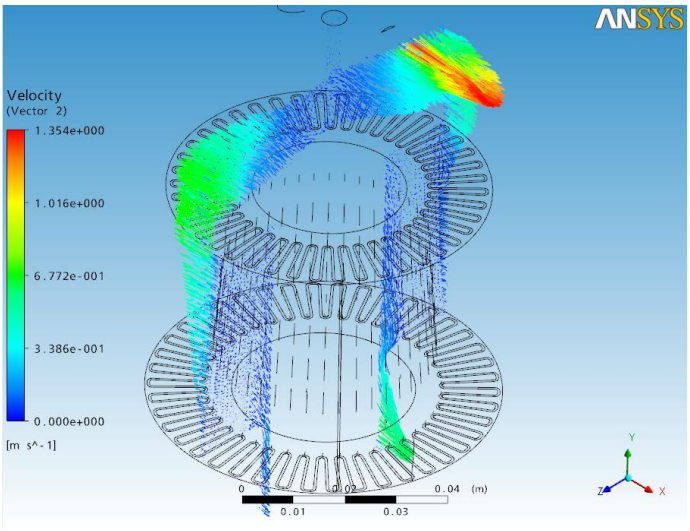

Figure 9 – Velocity vectors at plane N-S

Figures 10 shows velocity vectors along planes E and O. At plane E can be seen a flow direction change and a splitting at the inner bottom.

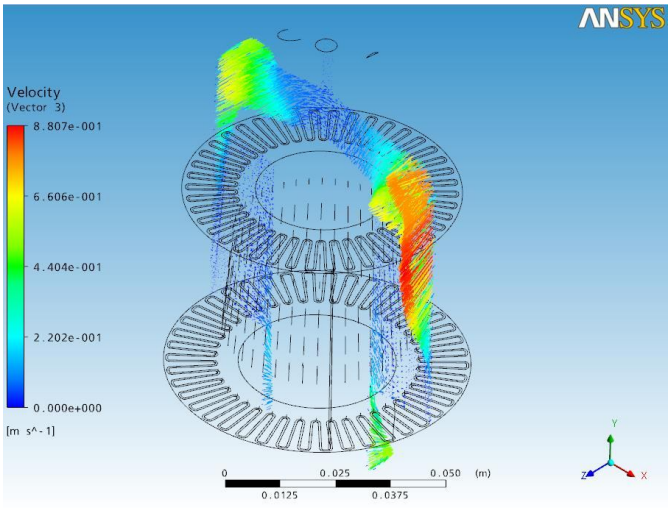

Figure 10 – Velocity vectors at plane E-O

Figure 11 shows pressure variation along the plane localized on the filter´s upper region. The plane was positioned along coordinate Y taking the entrance connector´s line as center basis. The pressure gradient shows a maximum value near the entrance and the space of each color indicates a constant variation. Therefore, the flow is fully developed in agree with the experimental data presented by Huebner [2003].

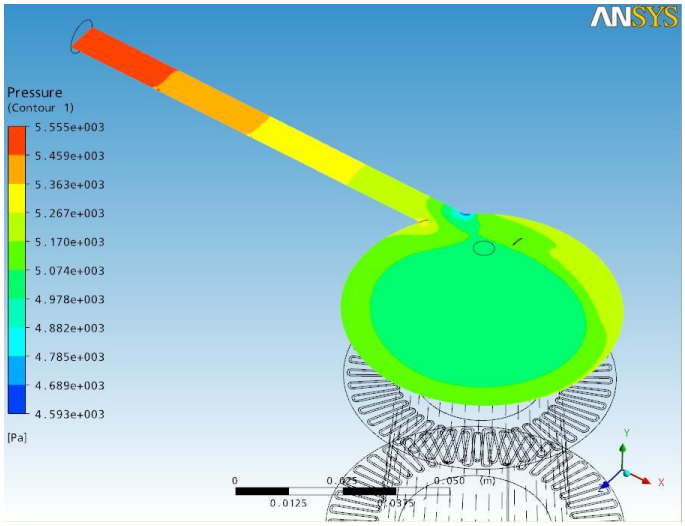

Figure 11. Pressure field on the upper plane.

Figure 12 show the pressure variation along planes N-S. It is observed that the pressure is greater at the region near the wall and it decreases at filter´s inner region.

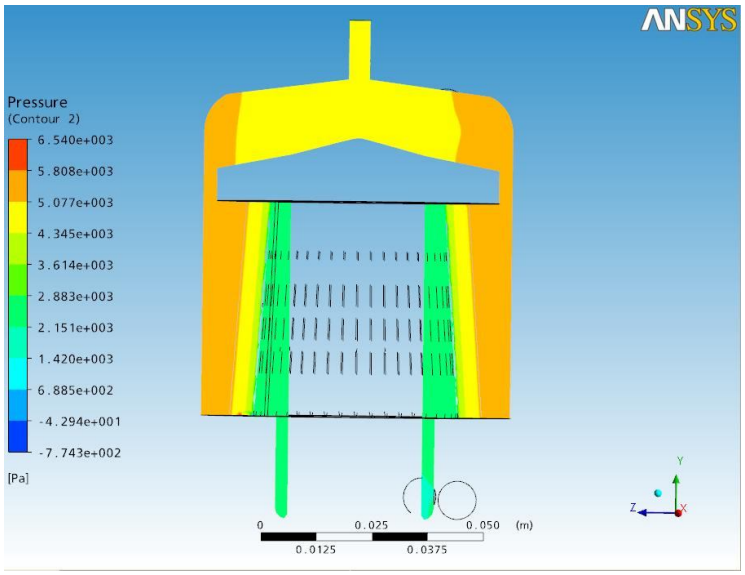

Figure 12 – Pressure field on plane N-S

Figures 13 and 14 show kinetic energy and dissipation distribution on the upper plane, respectively. The turbulent kinetic energy maximum value occurs at the region where the jet coming from the entrance hits the filter´s wall, forcing a flow change of direction. The dissipation has a maximum value at the entrance connector´s neighborhood where the flow is exposed to an expansion.

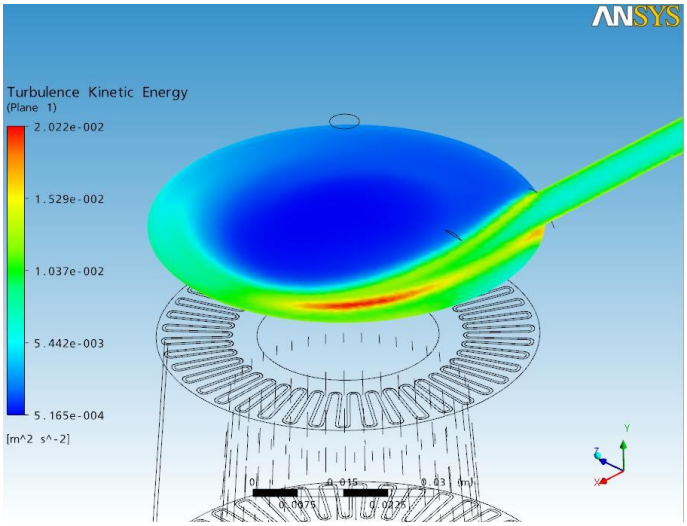

Figure 13 – Turbulent Kinetic energy on the upper plane

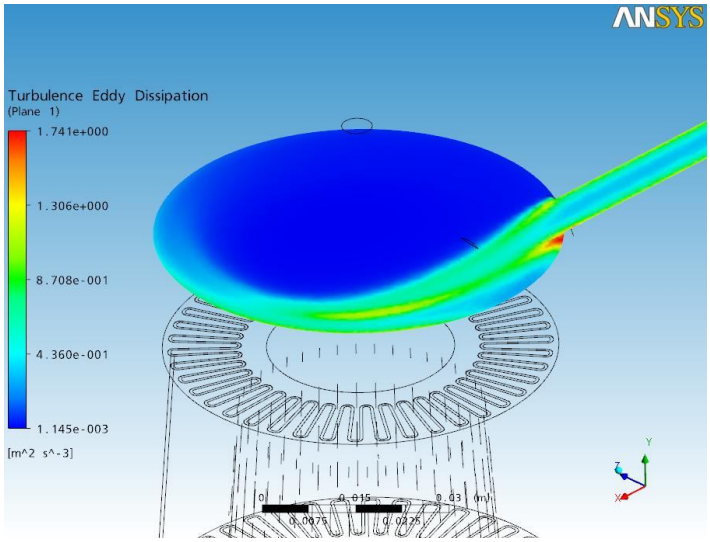

Figure 14 – Turbulent Eddy Dissipation on the upper plane

Similar results were obtained with an outflow of 1.5 and 3.0 l/min. Table 2 shows values of pressure drop obtained numerically and the percent variation compared with the results introduced by Huebner[2003].

Table 1. Numeric and experimental values of pressure drop

Outflow (l/min)	Numeric(Pa)	Experimental (Pa)	Difference (%)
1.5	1081	1039.65	3.98
3.0	2778	2777.75	0.01
4.5	5556	5443.54	2.07

The values show a maximum difference of 3.98% between numerical and experimental results. These results can be improved with a better correction of coefficients used on Darcy´s Law to model the pressure drop at the porous media. The results introduced along this work indicates that despite the difference between the numerical and experimental pressure drop the behavior of field flow follows the pattern obtained by Huebner [2003].

4. CONCLUSION

The present work presents results obtained from a numeric simulation of flow field along an arterial blood filter. The turbulence model the k-ε of two equations was used due to its robustness and convergence facility. The results regarding pressure drop present good agreement with data found on literature and the differences observed can be reduced by the adjust of Darcy law´s constant, used to simulate pressure drop on the filtering element. The flow field structure inside the blood filter was not fully reproduced by the numerical simulations this can be circumvented by the change of the turbulence model by one most appropriate to deal with recirculation as the k-ω SST model.

5. ACKNOWLEDGEMENTS

This work was financed by CNPq, processes n°200729/95-0 e n°300556/97-7. Acknowledgements to the support provided by FAPEMIG (Fundação de Amparo à Pesquisa de Minas Gerais) process TEC-APQ-01569-08.

6. REFERENCES

Andrade, A., Biscegli, J., Sousa, J.E., Ohashi, Y. & Nosé, Y. Flow visualization studies to improve the Spiral Pump Design, *Artificial Organs*, v.21, n.7, p.680-685, 1997.

Aris, A., Solanes, H., Cámara, M.L., Junqué, C., Escartin, A., e Caralps, J.M., Arterial line filtration during cardiopulmonary bypass, *J. Thorac. Cardiovasc. Surg.*, v.91, p.526-533, 1986.

Bergdahl, L., e Björk, V.O., The effect of a nylon mesh blood filter in the arterial line during extracorporeal circulation, *Scand. J. Cardiovasc. Surg.*, v.14, p.263-266, 1980

Burgreen, G.W., Loree II, H.M., Bourque, K., Dague, C., Poirier, V.L., Farrar, D., Hampton, E., Wu, Z.J., Gempp, T.M. e Schob, R., Computational fluid dynamics analysis of a maglev centrifugal left ventricular assist device, *Artificial Organs*, v.28, n.10, p.874-880, 2004.

Castellini, P., Pinotti, M. e Scalise, L., Particle Image Velocimetry for Flow Analysis in Longitudinal Planes across a Mechanical Artificial Heart Valve, *Artificial Organs*, v.28, n.5, p.507-510, 2004.

Chan, W.K., Wong, Y.W., Ong, W., Koh, S.Y. e Chong, V., Numerical investigation of the effects of the clearence gap between the inducer and impeller of an axial blood pump, *Artificial Organs*, v.29, n.3, p.250-258, 2005.

Chung, T.J., *Computational Fluid Dynamics*, Cambridge University Press, Cambridge, 2002.

Deschamps, C.J., 1998. "Modelos Algébricos e Diferenciais", Proceedings of the 1st Spring School of Transition and Turbulence, Vol. 1, Rio de Janeiro, Brazil, pp. 99-155.

Dewanjee, M.K., Palatianos, G.M., Kapadvanjwala, M., Novak, S., Hsu, L., Serafini, A.N. e Sfakianakis, G.N., Rate constants of embolization and quantitation of emboli from the hollow-fiber and arterial filter during cardiopulmonary bypass, *ASAIO Journal*, v.38, p.317-321, 1992.

Gage, K., Gartner, M.J., Burgreen, G.W. e Wagner, W.R., Predicting membrane oxygenator pressure drop using computational fluid dynamics, *Artificial Organs*, v.26, n.7, p.600-607, 2002.

Gartner, M.J., Wilhelm, C.R., Fabrizio, M.C. e Wagner, W.R., Modeling flow effects on thrombotic deposition in a membrane oxygenator, *Artificial Organs*, v.24, n.1, p.29-36, 2000.

Huebner, R., Tese de Doutorado – Escoamento em filtros de linha arterial utilizados em circuitos de circualação extracorpórea. Universidade Federal de Minas Gerais, Programa de Pós-Graduação em Engenharia Mecânica, 2003

Ilinca, F., Pelletier, D. and Garon, A., 1997. An adaptive finite element method for a two-equation turbulence model in wall-bounded flows. International Journal for Numerical Methods in Fluids, vol. 24, pp. 101–120.

Kim, W.G., Kim, K.B. e Yoon, C.J., Scanning microscopic analysis of arterial line filters used in cardiopulmonary bypass, *Artificial Organs*, v.24, n.11, p.874-878, 2000.

Mueller, X.M., Tevaearai, H.T., Jegger, D., Augstburger, M., Burki, M. e von Segesser, L.K., Ex vivo testing of the Quart arterial line filter. *Perfusion*, v.14, p.481-487, 1999.

Pinotti, M., Paone, N. Estimating mechanical blood trauma in centrifugal blood pump: LDA measurements of the mean velocity field. *Artificial Organs*, vol.20, n.6, p.546-552, 1996.

Untaroiu, A., Throckmorton, A.L., Patel, S.M., Wood, H.G., Allaire, P.E. e Olsen, D.B., Numerical and experimental analysis of an axial flow left ventricular assist device: The influence of the diffuser on overall pump performance, *Artificial Organs*, v.29, n.7, p.581-591, 2005.

Waaben, J., Sϕrensen, H.R., Andersen, U.L.S., Gefke, K., Lund, J., Aggestrup, S., Husum, B., Laursen, H., Gjedde, A. Arterial line filtration protects brain microcirculation during cardiopulmonary bypass in the pig", *The journal of Thoracic and Cardiovascular Surgery*, v.107, n.4, p.1030-1035, 1994.

7. RESPONSIBILITY NOTICE

The authors are the only responsible for the printed material included in this paper.